SCIENTIFIC REPORTS

OPEN

SUBJECT AREAS:
ELECTROCATALYSIS
CARBON NANOTUBES AND FULLERENES
FUEL CELLS
SELF-ASSEMBLY

Received
17 December 2012

Accepted
4 April 2013

Published
3 May 2013

Correspondence and requests for materials should be addressed to T.F. (fujigaya-tcm@mail.cstm.kyushu-u.ac.jp) or N.N. (nakashima-tcm@mail.cstm.kyushu-u.ac.jp)

Remarkably Durable High Temperature Polymer Electrolyte Fuel Cell Based on Poly(vinylphosphonic acid)-doped Polybenzimidazole

Mohamed R. Berber[1,4], Tsuyohiko Fujigaya[1,3], Kazunari Sasaki[2,3] & Naotoshi Nakashima[1,3,5]

[1]Department of Applied Chemistry, Graduate School of Engineering, Kyushu University, 744 Motooka, Nishi-ku, Fukuoka 819-0395, Japan, [2]Department of Mechanical Engineering Science, Graduate School of Engineering, Kyushu University, 744 Motooka, Nishi-ku, Fukuoka 819-0395, Japan, [3]International Institute for Carbon Neutral Energy Research (WPI-I2CNER), Kyushu University, Fukuoka 819-0395, Japan, [4]Department of Chemistry, Faculty of Science, Tanta University, Tanta 31527, Egypt, [5]JST-CREST, 5 Sanbancho, Chiyoda-ku, Tokyo, 102-0075, Japan.

Low durability of polymer electrolyte fuel cell (PEFC) is a major drawback that should be solved. Recent studies have revealed that leaching of liquid phosphoric acid (PA) from both polymer electrolyte membrane and catalyst layers causes inhomogeneous PA distribution that results in deterioration of PEFC performance during long-term operation. Here we describe the finding that a novel PEFC free from acid leaching shows remarkable high durability (single cell test: >400,000 cycling) together with a high power density at 120°C under a non-humidified condition. This is achieved by using a membrane electrode assembly (MEA) with Pt on poly(vinylphosphonic acid)-doped polybenzimidazole wrapped on carbon nanotube and poly(vinylphosphonic acid)-doped polybenzimidazole for the electrocatalst and electrolyte membrane, respectively. Such a high performance PEFC opens the door for the next-generation PEFC for "real world" use.

The polymer electrolyte fuel cell (PEFC) is one of the most promising power sources for cars and houses due to its high-energy conversion efficiency[1,2]. Recently, increasing attention has been received for higher temperature PEFC systems due to their several advantages[3]; namely, i) higher power efficiency can be realized, ii) the cooling device and water management system become unnecessary[4], iii) reduction of CO poisoning of the platinum (Pt) enables an elimination of a precise fuel gas purification[3,5,6] and iv) the high reactivity allows the use of a non-precious metal catalyst[7,8]. All of these factors also contribute to the high cost reduction.

In the current PEFC systems, water-assisted proton conduction in the conventional polyelectrolytes limit the operation temperature below 100°C[9]. The limitation of operating temperature originated from the poor proton conductivity of the conventional polyelectrolytes such as Nafion at temperatures above 100°C[9], thus the development of a new polyelectrolyte with a high proton conductivity at high temperature has been strongly desired. To overcome this temperature limitation problem, the use of polymer membrane doped with a non-volatile liquid acid as a polymer electrolyte membrane (PEM) has been proposed[10], in which the mobile acid such as phosphoric acid (PA) is responsible for the proton conduction through the vehicle mechanism. Especially, phosphoric acid-doped polybenzimidazoles (denoted PA-doped PBIs) have been considered as the most promising substitutive polyelectrolytes[11,12] and the PEFC employing PA-doped PBIs not only in PEM but also in the catalyst layers (Cat-L) have been developed for high temperature operation[10,13–15]. However, recent studies have revealed that leaching of liquid PA from PEM[16] and Cat-L[17] causes inhomogeneous PA distribution that results in deterioration of PEFC performance during long-term operation.

In this study, in order to prevent acid leaching from the high temperature PEFC system, we used poly(vinylphosphonic acid) (PVPA) in place of PA because PVPA is a polymeric acid and is stably bound to the PBIs via multipoint acid-base reactions[18]. We then carried out single cell durability test for a membrane-electrode assembly (MEA) fabricated from our materials. The PVPA is known to form a hydrogen-bonding network with the neighboring phosphonic acid groups[19,20]; consequently, it forms an effective proton pathway after blending with the PBIs, and the proton conductivity of PVPA-doped PBIs films has been reported to be $\sim 10^{-3}$ S. cm^{-1} at 50%

RH (80°C)[18,21]. In order to employ this idea to the PEFC system, a proper electrocatalyst design that satisfies the use of the minimized amount of the electrolyte in the Cat-L for smooth gas diffusion and effective proton conduction is highly important.

Here, we fabricated a novel electrocatalyst for Cat-L assembled with carbon nanotubes (CNTs)[22], PVPA-doped PBI and platinum (Pt) nanoparticles as an electron-conducting supporting material, electrolyte and metal catalyst, respectively. Bottom-up assembly of nanometer-thick PVPA-doped PBI layer around CNTs is expected to serve as an effective proton conduction pathway via the Grotthuss mechanism. The doping stability of PVPA in addition to the PEFC activity and durability were studied. This is the first report to employ PVPA-doped PBI not only for PEM but also for the electrocatalyst in Cat-L to fabricate the MEA and to operate the MEA under non-humidified condition at above 100°C.

Results

The electrocatalyst without the PVPA doping was prepared according to our previous report[23,24]. Briefly, poly[2,2′-(2,6-pyridine)-5,5′-bibenzimidazole] (PyPBI) non-covalently wrapped the surfaces of multi-walled carbon nanotubes (MWNTs) through a strong physical interaction, then Pt particles with a diameter of 3.15 ± 0.62 nm were immobilized onto the PyPBI layer (Fig. 1). Previously, the obtained electrocatalyst composite (MWNT/PyPBI/Pt) was employed in the MEA using PA-doped PBI film as PEM and showed high activity even without the doping in MWNT/PyPBI/Pt probably due to the doping by leached PA from the PEM[15]. This time, the obtained composite (MWNT/PyPBI/Pt) was doped with PVPA through a simple mixing of the MWNT/PyPBI/Pt with PVPA in an aqueous solution, and the PVPA doped composite (MWNT/PVPA-PyPBI/Pt) was obtained after removing the unbound PVPA by vigorous water rinsing (Fig. 2a). Fig. 2b shows photographs of the MWNT/PyPBI/Pt (left) and MWNT/PVPA-PyPBI/Pt (right) dispersed in water after a 5-min sonication. The MWNT/PVPA-PyPBI/Pt was found then to be well-dispersed in the solvent.

The X-ray photoelectron spectroscopy (XPS) diagram of the MWNT/PVPA-PyPBI/Pt was measured and the result is shown in Fig. 2c (red lines). The XPS result of the MWNT/PyPBI/Pt is also shown for comparison (black lines in Fig. 2c). The N_{1s} peak at 400 eV[25] and Pt_{4f} doublet peaks at 71.1 and 74.4 eV attributable to $Pt^0_{4f7/2}$ and $Pt^0_{4f5/2}$, respectively[26], were observed for both the MWNT/PyPBI/Pt and MWNT/PVPA-PyPBI/Pt, while the P_{2p} peak at 132 eV was detected only for the MWNT/PVPA-PyPBI/Pt.

Based on a thermogravimetric analysis (TGA), a weight-reduction of ca. 4 wt% in the range of 200 ~ 300°C attributed to the dehydration of the phosphonic acid group of PVPA (loss of water molecules from the adjacent phosphonic acids) as well as hydrated water from PVPA/PBI membrane (Fig. 2d) is observed[27]. In addition, due to the PVPA doping, the apparent weight ratio of the Pt determined from the weight residue at 900°C decreased from 47.8 to 43.7 wt%. Considering the total amount of the Pt in the MWNT/PyPBI/Pt remains even after the PVPA doping, the 4.1-wt% decrease corresponds to the 8.6-wt% addition of the PVPA in the MWNT/PVPA-PyPBI/Pt (Fig. 2e). From the TGA of the PVPA, it was roughly estimated that one water molecule is hydrated per one PVPA unit (see Supplementary Information, Fig. S1), and thus, an 8.6-wt% addition of PVPA is calculated to be 6.1-wt% dehydrated PVPA in the composite. Since the weight ratio of the PyPBI in the MWNT/PyPBI is 8 wt%[28], the weight ratio of the PyPBI in the MWNT/PVPA-PyPBI/Pt was calculated to be 3.8 wt%. Therefore, the total polymer content in the electrocatalyst is 9.9 wt% (6.1 + 3.8 wt%), which is much lower than that (>20 wt%) of the other systems[6,29,30].

Morphological insights of the composite after the PVPA doping were obtained from the direct observation by using a scanning electron microscope (SEM). Figs. 2f and 2g show typical SEM images of the MWNT/PyPBI/Pt and MWNT/PVPA-PyPBI/Pt, respectively. Bright spots from the Pt nanoparticles observed for the MWNT/PyPBI/Pt were hardly seen in the MWNT/PVPA-PyPBI/Pt; instead, a homogeneous polymer coating due to the PVPA was clearly recognized. We confirmed the presence of highly dispersed Pt nanoparticles inside the PVPA coating by scanning transmission electron microscope (STEM) measurements (see Supplementary Information, Fig. S2). For more details, the SEM and STEM images of the isolated MWNT/PyPBI/Pt and MWNT/PVPA-PyPBI/Pt are also provided in the Supplementary Information (see Supplementary Information, Fig. S3).

Cyclic voltammogram (CV) measurements on the PVPA-wrapped and non-wrapped composites were carried out in 0.1 M $HClO_4$ aqueous solutions[31,32]. The electrochemical surface area (ECSA) of the Pt nanoparticles of the MWNT/PVPA-PyPBI/Pt was evaluated to be 40.2 m^2/g, which is lower than that 51.6 m^2/g of the MWNT/PyPBI/Pt[23] (see Supplementary Information, Fig. S4).

As a PEM, the PVPA/PBI film was chosen in place of a PA-doped PBI membrane (which is typically used for PBI-based PEFC) in order to avoid the PA leaching to the Cat-L[33]. The impedance profile of the PVPA/PBI membrane at 120°C is displayed in Fig. S5a. The proton conductivity was calculated to be 0.0172 S. cm^{-1}, which is comparable to that of Nafion at 80°C under humidified conditions[34] and that of PA-doped PBI at 120°C under non-humidified conditions[35]. The temperature dependence of the conductivity at dry H_2 conditions is presented in Fig. S5b. The conductivity is highly increased above 80°C. To indicate the mechanism of the proton conduction, Fig. S5b is replotted to the Arrhenius plot (Fig. 3a), from which the activation energy of the proton conduction is calculated to be 53.3 kJ/mol. The mechanical toughness of the PVPA/PBI film was measured (see Supplementary Information, Fig. S6) and the obtained tensile strength was found to be 91.1 MPa. The addition of PVPA to PBI slightly decreased the tensile strength of PBI[36].

A fuel cell test was performed using a MEA prepared by assembling the electrocatalyst (MWNT/PVPA-PyPBI/Pt), and the PEM (PVPA/PBI film) (denoted PVPA-doped MEA). To examine the effect of the PVPA-doping in the electrocatalyst, two MEAs were fabricated as controls. One is composed of MWNT/PyPBI/Pt and PA-doped PBI as electrocatalyst and PEM, respectively (denoted PA-non-doped MEA), and the other is composed of MWNT/PyPBI/Pt and PVPA/PBI as electrocatalyst and PEM, respectively (denoted PVPA-non-doped MEA) (Table 1).

The PA-non-doped MEA possessed a similar composition to the state-of-the-art MEA in PBI-based PEFC, and it showed a power density of 180 mW/cm^2 (see Supplementary Information, Fig. S7).

The polarization and the power density curves of the PVPA-doped MEA and PVPA-non-doped MEA measured at 120°C without external humidification are shown in Fig. 3a. The open circuit voltages (OCV) of both MEAs were ~0.9 V, and the difference in the

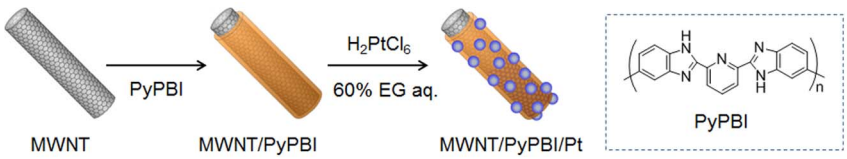

Figure 1 | Schematic illustration of the preparation technique of MWNT/PyPBI/Pt. Chemical structure of PyPBI is presented in the dotted frame.

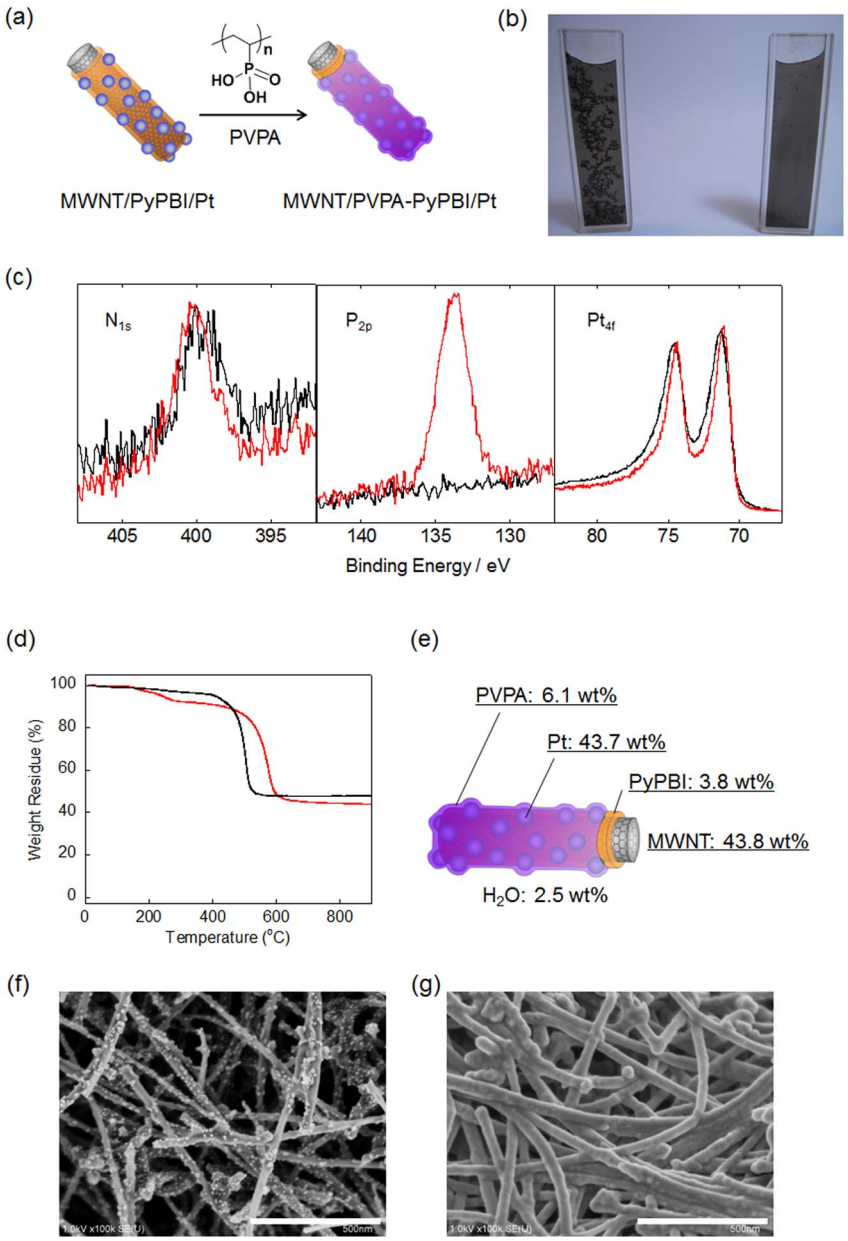

Figure 2 | Characterizations of PVPA coating for MWNT/PyPBI/Pt. (a), Schematic illustration of the preparation technique of the MWNT/PyPBI-PVPA/Pt. (b), Photographs of aqueous dispersion of the MWNT/PyPBI/Pt (left) and MWNT/PyPBI-PVPA/Pt (right) after sonication for 5 min. (c), XPS narrow scans of N_{1s} P_{2p} and Pt_{4f} regions for the MWNT/PyPBI/Pt (black line) and MWNT/PVPA-PyPBI/Pt (red line). (d), TGA curves for the MWNT/PyPBI/Pt (black line) and MWNT/PVPA-PyPBI/Pt (red line). (e) Composition analysis for the MWNT/PVPA-PyPBI/Pt calculated based on the TGA data. (f) SEM image of the MWNT/PyPBI/Pt. (g) SEM image of the MWNT/PVPA-PyPBI/Pt.

cell voltage became obvious upon increasing the applied current density. We found that the PVPA-doped MEA showed a higher cell voltage at all applied current densities. The maximum power density of the PVPA-doped MEA was 252 mW/cm^2, while that of the PVPA-non-doped MEA was as low as 20 mW/cm^2. Notably, the PVPA-doped MEA achieved a power density of around 75% of the maximum power even at 1600 mA/cm^2. This power value is remarkably high compared to other PBI-based PEFC systems measured at similar conditions[15].

Fig. 4 displayed the XPS spectra of the electrocatalyst collected from the delaminated PVPA-non-doped MEA (red line) and the delaminated PA-non-doped MEA (black line). The PVPA-non-doped MEA showed no detectable P_{2p} peaks, whereas for the PA-non-doped MEA, clear P_{2p} peaks are clearly detected.

The polarization curves of the PVPA-doped MEA (Fig. 5a) together with the PA-non-doped MEA (Fig. 5b) measured after every 40,000 cycles of the potential sweeps between 1.0 and 1.5 V were selected for display. The corresponded power density curves are presented in the supporting information (Fig. S8). The cell voltage at 200 mA/cm^2 for the polarization curves shown in Figs. 5a and 5b is plotted as a function of the cycle numbers (Fig. 5c). While the cell voltage of the PA-non-doped MEA (black circles in Fig. 5c) drastically decreased upon repeated cycling, that of the PVPA-doped MEA (red circles in Fig. 5c) exhibited a gradual decrease; namely, the high cell voltage is still remained even after 400,000 cycles. Fig. 5d displayed the power density curves of PVPA-doped MEA at different operating temperatures. As observed, the increase of the operating temperature increased the output power density.

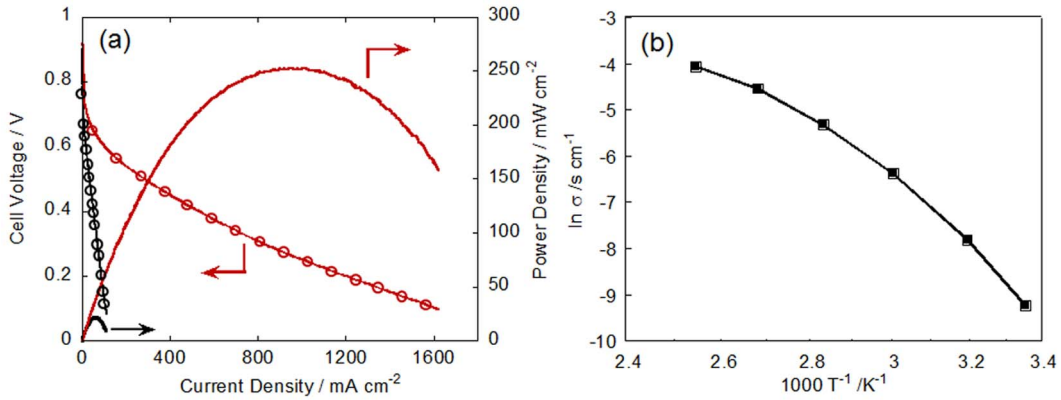

Figure 3 | Performance of MEAs. Polarization (line with open circles) and power density (bold line) curves of the PVPA-doped MEA (red line) and PVPA-non-doped MEA (black line) (a). Arrhenius plot of the proton conductivity of PVPA/PBI membrane (b).

Discussion

The photographs of Fig. 2b indicated a successful coating of the hydrophobic PyPBI layer by the PVPA through an acid-base reaction between the PVPA and PyPBI[18,37]. In addition, the XPS results of Fig. 2c confirmed the PVPA doping of the MWNT/PyPBI/Pt.

Generally, a higher loading of the polyelectrolyte leads to a higher proton conductivity, while thick coverage of the catalyst surfaces by the polyelectrolyte results in poor access of the fuel gases to the surfaces[38]. For this reason, a polyelectrolyte weight-reduction without reducing the proton conductivity is a key design strategy for a Cat-L with a high performance. Accordingly, the observed low polyelectrolyte content determined from TGA result (9.9 wt%) in our electrocatalyst has a significant advantage in such a high performance fuel cell catalyst design. The CV measurements showed a decrease in the ECSA after PVPA coating and this decrease might lead to a decrease in the accessible area for hydrogen. However, the amount of the polymer in our catalyst is lower than those of the other reported systems as already described. Therefore, the effect of the mass transfer hindrance is expected to be significantly low.

In fuel cell measurements, the higher performance of the PA-non-doped MEA (180 mW/cm^2) compared to the PVPA-non-doped MEA (20 mW/cm^2) can be explained by an *in-situ* doping of the electrocatalyst (MWNT/PyPBI/Pt) due to mobile PA molecules leached from the PEMs[16,17]. In other words, the observed very low power density (20 mW/cm^2) of the PVPA-non-doped MEA clearly shows the absence of acid-leaching in the PVPA-doped PEM system. Indeed, the absence of P_{2p} peaks in the XPS analysis of the Cat-L delaminated from the PVPA-non-doped MEA (Fig. 4) confirmed the free acid-leaching system.

In PBI, based on an acid-base reaction, only two PA molecules interact (react) with an imidazole unit per repeating unit of PBI; however, the PBI-based PEMs are typically doped with 4 ~ 10 PA molecules[10] because the unbound excess PA are responsible for the high proton conductivity[39]. Thus, PA-doped PEMs always involve the risk of PA leaching from the PEMs[10].

By considering the absence of the acid-leaching of PVPA-doped PEM together with the high proton conductivity of the PVPA/PBI membrane, the high power density (252 mW/cm^2) of the PVPA-doped MEA clearly manifested the presence of proton conductivity in the Cat-L MWNT/PVPA-PyPBI/Pt. Judging from the activation energy of the proton conduction for the PVPA/PBI membrane (53.3 kJ mol^{-1}, Fig. 3a), protons move through a hydrogen-bonding network of the PVPA bound to the PBI *via* the Grotthuss mechanism[40]. Hence, we assume that the hydrogen-bonding network of the PVPA in the Cat-L formed along the PyPBI-wrapped MWNTs participates in the smooth proton conduction to assure the reaction. Notably, the power density of 252 mW/cm^2 is comparable to those reported for PA-doped PBI MEAs measured under similar conditions[38,41]. This result suggests the successful replacement of the PA-doping system by a PVPA-doping system without reducing the activity of the MEA.

One may expect a high durability in such a leaching-free PBI-based MEA. Thus, we tested the durability of the PVPA-doped MEA by following the protocol proposed by the Fuel Cell Commercialization Conference of Japan (FCCJ)[42] (for details, see Supplementary Information, Fig. S9). As a comparison, the durability of a PA-non-doped MEA (MWNT/PyPBI/Pt electrocatalyst doped with leached PA) was tested. An extremely high durability was achieved by the PVPA doping of PBIs in both the PEM and the Cat-L, which are free from acid leaching (Fig. 5). Such high durability of PVPA-doped MEA shows an extended stability of PEM against degradation, and also shows a continuous connection of the proton path in the Cat-L that usually cause MEA deterioration[16,17].

Table 1 | The compositions of the MEAs in this study. MEA naming is based on the dopant used for PEM and the presence of PVPA-doping in the electrocatalyst

MEA name	PEM	Cat-L
PVPA-doped MEA	PVPA/PBI blend film	MWNT/PVPA-PyPBI/Pt
PVPA-non-doped MEA		MWNT/PyPBI/Pt
PA-non-doped MEA	PA-doped PBI film	MWNT/PyPBI/Pt

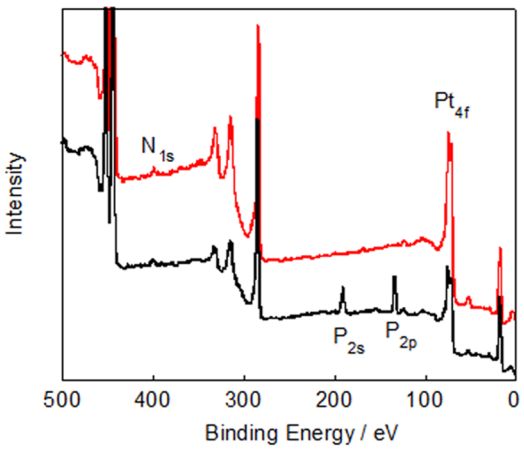

Figure 4 | Monitoring of the acid leaching using delaminated MEA. XPS spectra of the electrocatalyst collected from the PVPA-non-doped MEA (red line) and PA-non-doped MEA (black line).

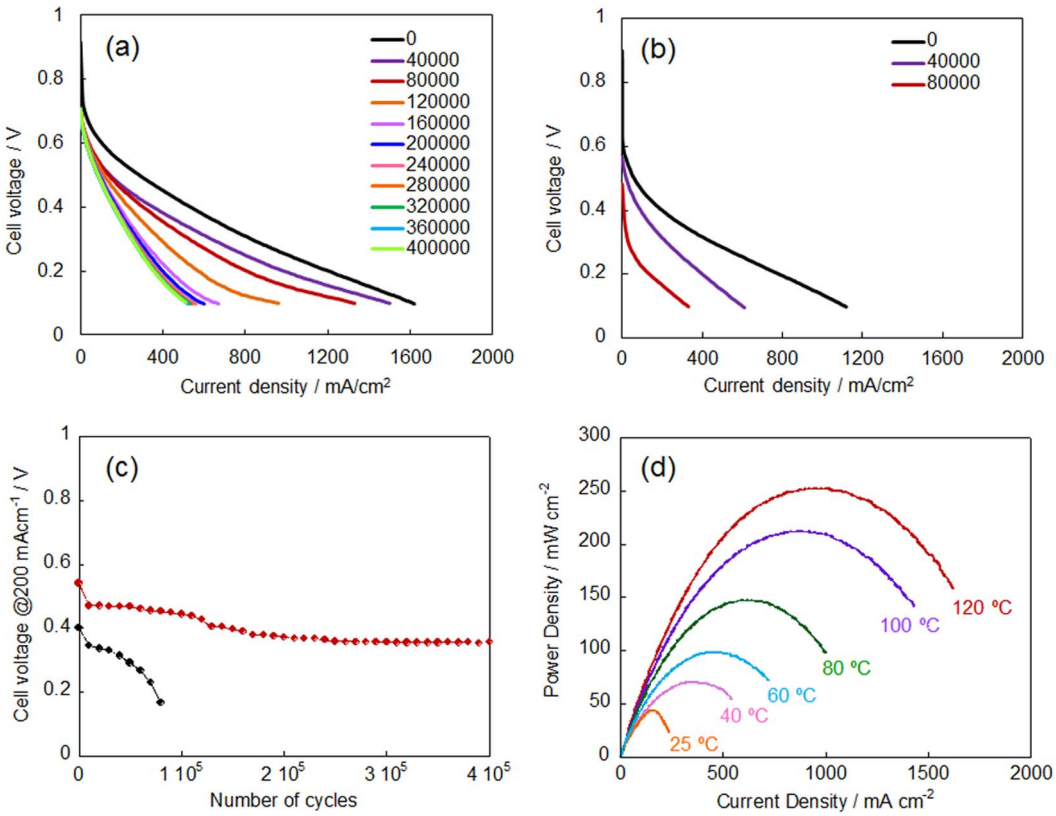

Figure 5 | Durability test of MEA. a. b, Polarization curves of a durability test using PVPA-doped MEA (a) and PA-non-doped MEA (b). The polarization curves were measured after every 1,000 cycles of the potential sweep between 1.0 and 1.5 V. For convenience, the data were plotted every 40,000 cycles. (c), Plots of the cell voltage at 200 mA/cm^2 for the PVPA-doped MEA (red line) and PA-non-doped MEA (black line). (d), Power density curves of the PVPA-doped MEA measured at 25°C (orange line), 40°C (pink line), 60°C (blue line), 80°C (green line), 100°C (purple line) and 120°C (red line).

Such a highly durable system is attractive for the use at high temperatures because higher temperatures always provide higher power efficiency than the conventional systems, and also is advantageous as a power source. As shown in Fig. 5d, the power density of our MEA increased when increasing the measurement temperature up to 120°C. The result is in good agreement with the increase of the proton conductivity at higher temperatures *via* the Grotthuss mechanism. Hence, a higher power density is expected above 120°C. This study is underway now by using a new apparatus capable of 120–200°C measurements.

In conclusion, we succeeded in the fabrication of a PBI-based MEA with a high activity and high durability using a polymeric acid dopant, PVPA, in place of a conventional monomeric acid dopant, PA, in which the PVPA-blended PBI (PVPA/PBI) and PVPA-doped MWNT/PyPBI/Pt composite (MWNT/PVPA-PyPBI/Pt) were used as the PEM and Cat-L, respectively. By employing PVPA instead of PA, the acid leaching, which is a crucial problem in the current PBI-based PEFC system, is successfully suppressed. Quite importantly, our PBI-based MEA showed a high activity even in the absence of the acid-leaching at a high operating temperature without external humidification. We found that the PVPA hydrogen-bonding network of PVPA is well developed through the membrane and the Cat-L, facilitating an efficient proton delivery *via* the Grotthuss mechanism. Moreover, our MEA exhibited an extremely high durability compared to the PA-doped PEFCs due to the stable PVPA doping in the MEA and Cat-L through multi-point acid-base reactions. The modification of PVPA/PBI blend ratio and/or the operation temperature is expected to improve the performance of the MEA.

The present study opens the door for the next-generation high temperature and non-humidified PEFC for use in the "real world".

Methods

Materials. *N,N*-Dimethylacetamide (DMAc), ethylene glycol (EG), hydrogen hexachloroplatinate hexahydrate ($H_2PtCl_6 \cdot 6H_2O$), and poly(vinylphosphonic acid) (PVPA) were purchased from Wako Pure Chemical, Ltd., and used as received. Multi-walled carbon nanotubes (MWNTs; ca. 20 nm diameter) were kindly provided by the Nikkiso Co. Poly[2,2′-(2,6-pyridine)-5,5′-bibenzimidazole] (PyPBI) and poly[2,2′-(2,6-phenyl)-5,5′-bibenzimidazole] (PBI) were synthesized according to previously reported methods[43]. The MWNT wrapped with PyPBI (MWNT/PyPBI) and their Pt composite (MWNT/PyPBI/Pt) were prepared based on our previous report[23].

Preparation of MWNT/PVPA-PyPBI/Pt electrocatalysts. The MWNT/PyPBI/Pt composite (10 mg) was added to an aqueous solution of EG (10 mL). The mixture was sonicated using a bath-type sonicator (BRANSON 5510) for 5 min, and then stirred for 1 h, to which 1 mL of a PVPA solution (30%) was added. The resultant mixture was stirred for 1 h at room temperature followed by filtration, rinsing with water, and then vacuum drying.

Preparation of PVPA/PBI blend membrane. The PVPA/PBI membrane was prepared in the blend ratio of 1 : 1 (mol/mol) with respect to the monomer repeating unit of PVPA and PBI. This ratio was chosen because it provided an evident structured resonance from the hydrogen-bonded protons that exhibits the lowest activation energy for proton mobility[18]. In a 50 mL glass bottle, LiBr (100 mg) was dissolved in DMAc (10 mL) to which PBI (200 mg) and PVPA (70.1 mg) were added, then the mixture was stirred for 1 h. The resultant mixture was cast on a glass plate using a film applicator (Elcometer 3600, 50 mm strip width). The solvent was then gradually evaporated upon heating to 120°C, and maintained at that temperature for 5 h to completely remove the solvent. The film was peeled off the substrate, and then immersed in hot Milli-Q water to remove the LiBr. The membrane thickness was ~30 μm.

Materials characterization. X-ray photoelectron spectroscopy (XPS) spectra were measured using an AXIS-ULTRA^{DLD} (Shimadzu). Thermogravimetric analysis (TGA) measurements were conducted with a TGA-50 (Shimadzu) at the heating rate of 10°C/min under 20 mL/min flowing air. The SEM and STEM images were taken by SU8000 (Hitachi High-Tech) and SU9000 (Hitachi High-Tech, acceleration voltage of 30 kV) electron microscopes, respectively. A copper grid with a carbon support

(Okenshoji) was used for the TEM observations. The mechanical properties of the films were measured at 25°C using an EZ-S (Shimadzu) at a displacement rate of 1.0 mm min^{-1}. The typical size of the specimen was 20 mm, 10 mm and 33 μm in length, width and thickness, respectively. Three specimens were tested for reproducibility.

Proton conductivity measurements. The Proton conductivity of PVPA/PBI membrane was measured under dry H_2 using a four-point-probe conductivity cell attached to an electrochemical impedance spectrometer (Solartron 1287/1260 potentiostat/frequency response analyzer) equipped with Zplot software.

Electrochemical measurements. Electrochemical measurements were performed using a rotating ring disk electrode (RRDE-3; Bioanalytical Systems, Inc.) with a conventional three-electrode single cell at room temperature. A glassy carbon electrode (GC) with a geometric surface area of 0.282 cm^2 was used as the working electrode. A Pt wire and an Ag/AgCl were used as the counter and reference electrodes, respectively. The Ag/AgCl reference electrode was calibrated against the reference hydrogen electrode (RHE) potential in 0.1 M $HClO_4$. The potential of the sample electrode was controlled by a potentiostat (Model DY2323; ALS). Typically, the catalyst suspension was prepared as follows. A powder sample of the catalyst (1.0 mg) was ultrasonically dispersed in a 60% EG aqueous solution (2.0 mL) to form a homogeneous suspension. The suspensions of the MWNT/PyPBI/Pt (17.6 μL) and MWNT/PVPA-PyPBI/Pt (20.8 μL) were then cast onto GC electrodes, then air-dried. The cyclic voltammograms (CVs) of the electrocatalysts were measured in an N_2-saturated 0.1 M $HClO_4$ to determine the electrochemical surface areas (ECSAs).

Fuel cell testing. The MEA was fabricated as follows. The composite of the MWNT/PVPA-PyPBI/Pt was ultrasonically dispersed in an EG/water mixture, and then deposited on a gas diffusion layer (GDL) (SIGRACET gas diffusion media, GDL 25 BC, SGL Carbon Group) by vacuum filtration. The GDL was used as a filter to obtain a gas diffusion electrode (GDE). The PVPA/PBI blend membrane (molar ratio 1 : 1) was laminated between the two MWNT/PVPA-PyPBI/Pt GDEs to fabricate the PVPA-doped MEA. The PVPA-doped MEA was then hot-pressed at 120°C and 5 MPa for 30 s. In a similar way, a control MEA (PVPA-non-doped MEA), in which the MWNT/PyPBI/Pt was used as an electrocatalyst was fabricated. The performance of the assembled MEAs was measured at 120°C using a computer-controlled fuel cell test system (Model 890e, Scribner Associate, Inc.). The polarization curves were recorded at atmospheric pressure under flowing dry hydrogen (flow rate; 100 mL/min) and dry air (flow rate; 200 mL/min) at the anode and cathode, respectively.

Durability test. The assembled MEAs were subject to accelerating durability tests following the protocol provided by the Fuel Cell Commercialization of Japan (FCCJ). Typically, the potential sweeps were cycled between 1.0 and 1.5 V at 120°C under non-humidified conditions in order to accelerate the oxidation process. The scanning rate was 0.5 V/s. H_2 and N_2 were fed to the anode and the cathode, respectively. The I–V curves were recorded every 1,000 cycle after switching the cathode gas from N_2 to air. The potential was plotted as a function of cycling at 200 mA/cm^2. The 200 mA/cm^2 region is chosen since this current density is often used for the stationary PEFC[44].

1. Kirubakaran, A., Jain, S. & Nema, R. K. A review on fuel cell technologies and power electronic interface. *Renewable and Sustainable Energy Rev.* **13**, 2430–2440 (2009).
2. Wang, Y., Chen, K. S., Mishler, J., Cho, S. C. & Adroher, X. C. A review of polymer electrolyte membrane fuel cells: Technology, applications, and needs on fundamental research. *Appl. Energy* **88**, 981–1007 (2011).
3. Leikin, A., Bulycheva, E., Rusanov, A. & Likhachev, D. High-temperature proton-exchange membranes based on polymer-acid complexes. *Polym. Sci. Series B* **48**, 144–151 (2006).
4. Li, Q., He, R., Jensen, J. O. & Bjerrum, N. J. Approaches and Recent Development of Polymer Electrolyte Membranes for Fuel Cells Operating above 100°C. *Chem. Mater.* **15**, 4896–4915 (2003).
5. Yang, C., Costamagna, P., Srinivasan, S., Benziger, J. & Bocarsly, A. B. Approaches and technical challenges to high temperature operation of proton exchange membrane fuel cells. *J. Power Sources* **103**, 1–9 (2001).
6. Li, Q., He, R., Gao, J.-A., Jensen, J. O. & Bjerrum, N. J. The CO Poisoning Effect in PEMFCs Operational at Temperatures up to 200°C. *J. Electrochem. Soc.* **150**, A1599–A1605 (2003).
7. Zhang, J. *et al.* High temperature PEM fuel cells. *J. Power Sources* **160**, 872–891 (2006).
8. Parthasarathy, A., Srinivasan, S., Appleby, A. J. & Martin, C. R. Temperature Dependence of the Electrode Kinetics of Oxygen Reduction at the Platinum/Nafion® Interface---A Microelectrode Investigation. *J. Electrochem. Soc.* **139**, 2530–2537 (1992).
9. Zhang, H. & Shen, P. K. Recent Development of Polymer Electrolyte Membranes for Fuel Cells. *Chem. Rev.* **112**, 2780–2832 (2012).
10. Asensio, J. A., Sanchez, E. M. & Gomez-Romero, P. Proton-conducting membranes based on benzimidazole polymers for high-temperature PEM fuel cells. A chemical quest. *Chem. Soc. Rev.* **39**, 3210–3239 (2010).
11. Mecerreyes, D. *et al.* Porous Polybenzimidazole Membranes Doped with Phosphoric Acid: Highly Proton-Conducting Solid Electrolytes. *Chem. Mater.* **16**, 604–607 (2004).
12. Mamlouk, M. & Scott, K. Phosphoric acid-doped electrodes for a PBI polymer membrane fuel cell. *Int. J. Energy Research* **35**, 507–519 (2011).
13. Quartarone, E. & Mustarelli, P. Polymer fuel cells based on polybenzimidazole/H_3PO_4. *Energy Envison. Sci.* **5**, 6436–6444 (2012).
14. Li, Q., Jensen, J. O., Savinell, R. F. & Bjerrum, N. J. High temperature proton exchange membranes based on polybenzimidazoles for fuel cells. *Prog. Polym. Sci.* **34**, 449–477 (2009).
15. Matsumoto, K., Fujigaya, T., Sasaki, K. & Nakashima, N. Bottom-up design of carbon nanotube-based electrocatalysts and their application in high temperature operating polymer electrolyte fuel cells. *J. Mater. Chem.* **21**, 1187 (2011).
16. Oono, Y., Fukuda, T., Sounai, A. & Hori, M. Influence of operating temperature on cell performance and endurance of high temperature proton exchange membrane fuel cells. *J. Power Sources* **195**, 1007–1014 (2010).
17. Oono, Y., Sounai, A. & Hori, M. Influence of the phosphoric acid-doping level in a polybenzimidazole membrane on the cell performance of high-temperature proton exchange membrane fuel cells. *J. Power Sources* **189**, 943–949 (2009).
18. Akbey, Ü., Graf, R., Chu, P. P. & Spiess, H. W. Anhydrous poly(2,5-benzimidazole)-poly(vinylphosphonic acid) acid - base polymer blends: A detailed solid-state NMR investigation. *Aust. J. Chem.* **62**, 848–856 (2009).
19. Lee, Y. J. *et al.* High-resolution solid-state NMR studies of poly(vinyl phosphonic acid) proton-conducting polymer: Molecular structure and proton dynamics. *J. Phys. Chem. B* **111**, 9711–9721 (2007).
20. Yan, L., Feng, Q., Xie, L. & Zhang, D. About the choice of protogenic group for polymer electrolyte membranes: Alkyl or aryl phosphonic acid? *Solid State Ionics* **190**, 8–17 (2011).
21. Acar, O., Sen, U., Bozkurt, A. & Ata, A. Proton conducting membranes based on Poly(2,5-benzimidazole) (ABPBI)–Poly(vinylphosphonic acid) blends for fuel cells. *Int. J. Hydrogen Energy* **34**, 2724–2730 (2009).
22. Kato, Y., Inoue, A., Niidome, Y. & Nakashima, N. Thermodynamics on Soluble Carbon Nanotubes: How Do DNA Molecules Replace Surfactants on Carbon Nanotubes? *Scientific Report*, **2**, article number: 733 (2012).
23. Fujigaya, T., Okamoto, M. & Nakashima, N. Design of an assembly of pyridine-containing polybenzimidazole, carbon nanotubes and Pt nanoparticles for a fuel cell electrocatalyst with a high electrochemically active surface area. *Carbon* **47**, 3227–3232 (2009).
24. Okamoto, M., Fujigaya, T. & Nakashima, N. Design of an Assembly of Poly(benzimidazole), Carbon Nanotubes, and Pt Nanoparticles for a Fuel-Cell Electrocatalyst with an Ideal Interfacial Nanostructure. *Small* **5**, 735–740 (2009).
25. Hamilton, L. E., Sherwood, P. M. A. & Reagan, B. M. X-Ray Photoelectron-Spectroscopy Studies of Photochemical Changes in High-Performance Fibers. *Applied Spectroscopy* **47**, 139–149 (1993).
26. Tian, Z. Q., Jiang, S. P., Liang, Y. M. & Shen, P. K. Synthesis and Characterization of Platinum Catalysts on Multiwalled Carbon Nanotubes by Intermittent Microwave Irradiation for Fuel Cell Applications. *J. Phys. Chem. B* **110**, 5343–5350 (2006).
27. Samms, S. R., Wasmus, S. & Savinell, R. F. Thermal stability of proton conducting acid doped polybenzimidazole in simulated fuel cell environments. *J. Electrochem. Soc.* **143**, 1225–1232 (1996).
28. Fujigaya, T., Uchinoumi, T., Kaneko, K. & Nakashima, N. Design and synthesis of nitrogen-containing calcined polymer/carbon nanotube hybrids that act as a platinum-free oxygen reduction fuel cell catalyst. *Chem. Commun.* **47**, 6843–6845 (2011).
29. Pan, C. *et al.* Preparation and operation of gas diffusion electrodes for high-temperature proton exchange membrane fuel cells. *J. Power Sources* **172**, 278–286 (2007).
30. Kim, H.-J. *et al.* Polybenzimidazoles for high temperature fuel cell applications. *Macromol. Rapid Commun.* **25**, 1410–1413 (2004).
31. Thomas, S., Sung, Y. E., Kim, H. S. & Wieckowski, A. Specific Adsorption of a Bisulfate Anion on a Pt(111) Electrode. Ultrahigh Vacuum Spectroscopic and Cyclic Voltammetric Study. *J. Phys. Chem.* **100**, 11726–11735 (1996).
32. Labuda, A. *et al.* Switching Atomic Friction by Electrochemical Oxidation. *Langmuir* **27**, 2561–2566 (2011).
33. Oh, H.-S., Cho, Y., Lee, W. H. & Kim, H. Modification of electrodes using Al_2O_3 to reduce phosphoric acid loss and increase the performance of high-temperature proton exchange membrane fuel cells. *J. Mater. Chem. A* **1**, 2578–2581 (2013).
34. Sone, Y., Ekdunge, P. & Simonsson, D. Proton Conductivity of Nafion 117 as Measured by a Four-Electrode AC Impedance Method. *J. Electrochem. Soc.* **143**, (1996).
35. Ma, Y.-L., Wainright, J. S., Litt, M. H. & Savinell, R. F. Conductivity of PBI Membranes for High-Temperature Polymer Electrolyte Fuel Cells. *J. Electrochem. Soc.* **151**, (2004).
36. Zhang, L., Ni, Q.-Q., Shiga, A., Fu, Y. & Natsuki, T. Synthesis and mechanical properties of polybenzimidazole nanocomposites reinforced by vapor grown carbon nanofibers. *Polym. Composites* **31**, 491–496 (2010).
37. Aslan, A. & Bozkurt, A. Development and characterization of polymer electrolyte membranes based on ionical cross-linked poly(1-vinyl-1,2,4 triazole) and poly(vinylphosphonic acid). *J. Power Sources* **191**, 442–447 (2009).
38. Seland, F., Berning, T., Borresen, B. & Tunold, R. Improving the performance of high-temperature PEM fuel cells based on PBI electrolyte. *J. Power Sources* **160**, 27–36 (2006).

39. He, R., Che, Q. & Sun, B. The acid doping behavior of polybenzimidazole membranes in phosphoric acid for proton exchange membrane fuel cells. *Fibers Polym.* **9**, 679–684 (2008).
40. Suzuki, K., Iizuka, Y., Tanaka, M. & Kawakami, H. Phosphoric acid-doped sulfonated polyimide and polybenzimidazole blend membranes: high proton transport at wide temperatures under low humidity conditions due to new proton transport pathways. *J. Mater. Chem.* **22**, 23767–23772 (2012).
41. Kongstein, O. E., Berning, T., Borresen, B., Seland, F. & Tunold, R. Polymer electrolyte fuel cells based on phosphoric acid doped polybenzimidazole (PBI) membranes. *Energy* **32**, 418–422 (2007).
42. Ohma, A., Shinohara, K., Iiyama, A., Yoshida, T. & Daimaru, A. Membrane and Catalyst Performance Targets for Automotive Fuel Cells by FCCJ Membrane, Catalyst, MEA WG. *ECS Transactions* **41**, 775–784 (2011).
43. Carollo, A. *et al.* Developments of new proton conducting membranes based on different polybenzimidazole structures for fuel cells applications. *J. Power Sources* **160**, 175–180 (2006).
44. Wu, J. *et al.* A review of PEM fuel cell durability: Degradation mechanisms and mitigation strategies. *J. Power Sources* **184**, 104–119 (2008).

Acknowledgements

This work was supported in part by the Low-Carbon Research Network (LCnet) and the Nanotechnology Platform Project (Molecules and Materials Synthesis) of the Ministry of Education, Culture, Sports, Science and Technology (MEXT), Japan. The authors thank Ms. Zhiyun Noda and Mr. Kohei Kanda for technical assistance and useful discussions.

Author contributions

T.F. and N.N. proposed and supervised the project. M.R.B. carried out experiments. M.R.B., T.F., K.S. and N.N. discussed in detail about the obtained results. M.R.B., T.F. and N.N. wrote the manuscript.

Additional information

Supplementary information accompanies this paper at http://www.nature.com/scientificreports

Competing financial interests: The authors declare no competing financial interests.

License: This work is licensed under a Creative Commons Attribution-NonCommercial-NoDerivs 3.0 Unported License. To view a copy of this license, visit http://creativecommons.org/licenses/by-nc-nd/3.0/

How to cite this article: Berber, M.R., Fujigaya, T., Sasaki, K. & Nakashima, N. Remarkably Durable High Temperature Polymer Electrolyte Fuel Cell Based on Poly(vinylphosphonic acid)-doped Polybenzimidazole. *Sci. Rep.* **3**, 1764; DOI:10.1038/srep01764 (2013).